Accepted Manuscript

Appropriateness of Gait Analysis for Biometrics: Initial Study Using FDA Method

Kateřina Sulovská, Eva Fišerová, Martina Chvosteková, Milan Adámek

Appropriateness of Gait Analysis for Biometrics: Initial Study Using FDA Method

Kateřina Sulovská[a]*, Eva Fišerová[b], Martina Chvosteková[c], Milan Adámek[d]

[a] Tomas Bata University in Zlín, Faculty of Applied Informatics, CEBIA-Tech, Nad Stráněmi 4511, 760 05 Zlín, Czech Republic

[b] Palacký University, Faculty of Science, Department of Mathematical Analysis and Applications of Mathematics, 17 listopadu 12, 771 46 Olomouc, Czech Republic

[c] Slovak Academy of Sciences, Institute of Measurement Science, Dúbravská cesta 9, 841 04 Bratislava, Slovakia

[d] Tomas Bata University in Zlín, Faculty of Applied Informatics, Department of Security Engineering, Nad Stráněmi 4511, 760 05 Zlín, Czech Republic

* corresponding author: sulovska@fai.utb.cz

Abstract – Human body movement has been under continuous research for many years due to its potential application as a novel biometric system to identify individuals. It is possible to utilize various techniques, not only to obtain requested movement data, but also to analyse movement data. This paper uses functional data analysis on data obtained from 12 volunteers and uses 20 markers from the 3D motion capture system VICON MX T020. The functional data analysis was chosen as a suitable tool to obtain more information about an individual's movement because it uses a technique for real-time data, which corresponds to continuous time process. The results show that all markers, under any walking speed and condition, identify a significantly high percentage of individual pairs. Further, our results discriminate between markers, where some markers are highly dependent on walking speed and condition, and also on the influence of body part asymmetry. In addition, regular movement patterns in almost all participants' data shows a potential to identify individuals based on gait recognition with a 1:1 matching result.

Index Terms – Biometrics, functional data analysis, gait recognition, machine vision, pattern recognition.

I. INTRODUCTION

Human body movement and its analysis (i.e. behaviour of an individual during their bipedal locomotion) is an emerging commercially feasible behavioural biometric method [1–4], which nowadays is thoroughly studied at many research facilities all over the world. The bipedal locomotion is said to be unique for each person, and under stereotypical ideal conditions, undergoes only minimum changes throughout life, and it begins at the age of 9 [5]. Human body movement is widely used in everyday life in cases of reduced visibility (e.g. in tunnels or dark hallways), or by people with sight disabilities, when a passing person is naturally identified by their movement. This ability of the brain is now applied as a template for developing an automated recognition/identification (biometric) system. Over the years, research was focused on many short-term studies that were dedicated to the health sector (fall prevention [6], disease prevention [7], treatment evaluation [8] etc.), veterinary care [9],

robotics [10], static and dynamic features and their utilization [11–13], or to security [2]. Unfortunately, none of these studies focuses on a longitudinal study of entire human body movement of a wide sample of individuals (e.g. 1000+), intended especially for security purposes. However, some studies focused on smaller body parts (e.g. legs, arms or feet) and smaller samples of individuals (e.g. 15/105/120 people) and they presented valid results. It is possible to study body segments and joints, use the silhouette and/or trajectory analysis, and to successfully distinguish amongst a small group of people. However, some researchers admit doubts that selected methods and algorithms are inadequate for practical use in human recognition [13–17]. Research nowadays is very time-demanding, not only due to the development of novel algorithms that answer practical issues with video-based recognition, but also because contemporary algorithms must be properly used. In addition to this, in some cases it takes great time to acquire 2D & 3D data and studies are lengthy because of pre- and post-processing of data, including statistical analyses.

Commonly used methods for acquiring and studying the variability of the human gait contain video-based scanning or 3D motion capture systems [2,4,18–20], and different techniques or systems are used [20-21]. The most precise measurements are taken by 3D motion capture optoelectronic systems (e.g. VICON, QUALYSIS, BTS SMART), where the measurement accuracy is closer than 1 mm for each selected point (i.e. each marker on a selected body part – see Fig. 1). These systems usually use four cameras with infrared irradiation, highly sensitive sensors, and strobes that are capable of exceptional versatility that capture rapid and imperceptible movements. Together with the algorithms used, they are able to calculate entire movements (given by body segments labelled with retro-reflexive markers) in 3-dimensions. The most time-demanding part of this 3D-based analysis, also presented in this paper, is the data pre-processing and post-processing, where the focus is usually on thorough analysis of each gait signature [22-23]. This analysis is very important mainly for security applications (especially forensic applications), where proper statistical analysis is essential because it may be a question of life or death.

The human gait (i.e. bipedal locomotion) is a periodic movement of the whole body. This period of walking is called a double-step, or a gait cycle. The double-step consists of one right leg and one left leg step (i.e. from the right leg first heel contact to the second heel contact of the same leg). Each double-step is composed of unique walking characteristics, thus forming the gait signature. Generally, the average walking speed is approximately one double-step per second. However, there is a huge variance between individuals and a person's length of double-step can change even in consecutive cycles. The human body (in our case the set of retro-reflexive markers) generates the gait signature (i.e. trajectories) by moving through the space (depicted as curves when plotted) that represents the movement of the individual.

Commonly used statistical methods for studying the variability of the human gait include the MANOVA, ANOVA, or ANCOVA, the Kruskal-Wallis test, the Shapiro-Wilk test, the Kolmogorov-Smirnov test, the Tuckey HSD test, correlation coefficient calculations, Euclidean distances, multivariate data analysis, and also Fourier transformations [25–27]. In this paper, a different approach is presented which is based on Functional Data Analysis (FDA). In the FDA approach, each gait signature of the chosen marker from the dataset is considered a single entity [27-28]. These gait signatures are periodic, smooth, and interacting functions. Utilizing such analysis is appropriate in order to obtain the proper information that leads to greater algorithm stability, mainly for security purposes. This is important not only

because there is a need for great accuracy and reliability of the entire automated system, but it is important also to minimize the possibility of mixed-up or same body signatures between individuals in the database (caused e.g. by normalization and averaging of gait signatures, which occurs even in smaller datasets (e.g. [25]). The commonly used statistical analyses do not properly respect the functional character of the gait's behaviour, and therefore can omit some prerequisite data, which is crucial for proper analysis and results.

The applications involving human body movement analysis are mainly for rehabilitation, proper treatment, and monitoring a patient's state of health [7,9,18,29–31]. These applications prove that all of the benefits of motion capture systems positively affect human health and life. When considering security applications, the intended utilization of fully automated systems (based on video recognition/identification) is to monitor people at airports, banks, rows, stadiums, concourses, or near secured buildings (i.e. executive departments, courts etc..). Such systems can also be employed with the functional biometric system (e.g. face recognition, gait recognition or multi-modal systems), serving as a tool for forensic applications and a tool of commercial biometrics for companies [25,32,33]. Nowadays, several methods are used for identifying human body movement in order to test the practicality of each identification system (e.g. [34,35]) based on video records, whose main task is to identify and track human movement, mostly without directly identifying the individual. The main issue in order to decide which human locomotion analysis to use in the commercial security field and forensics is whether the system or technique is accurate enough, reliable, steady, and indisputable under various conditions and time.

This paper represents an initial study focused on the gait behaviour of volunteers while they perform different types of walking and this study will be considered as a prospective biometric identification method (used in the security sphere) that uses the FDA for statistical analysis. To obtain very accurate data in order for the FDA method to be meaningful, the 3D optoelectronic system was utilized by acquiring 2D data in the sagittal plane. The FDA method is employed to test common and specific traits of the entire movement of an individual in order to prove functionality and aptness of the gait analysis in terms of biometrics.

More precisely, the study deals mainly with the following issues: proving/disproving the effects of different walking speeds and conditions on human body movement patterns (movement signatures), distinguishing individual pairs based on gait signatures, evaluating markers' quality and also verifying the possibility of individuals' identification based on the gait recognition with a 1:N matching result. Obtaining answers for these above-mentioned issues will show how appropriate the gait analysis is as a tool for identifying/verifying a person in terms of biometrics/security analysis.

II. Methodology

A. *Experimental Settings & Data Acquisition*

All 12 volunteers (3 women and 9 men; see Table 1) took part in laboratory measurement experiments on the 3D motion capture optoelectronic system VICON MX T020. Participants did not state any problems in their muscular-skeletal system affecting their movement pattern.

The experiment measurements took place in the Gait Lab at the University Hospital Brno, the Czech Republic. All participants signed informed consent.

Figure 1. An example of the experiment measurements in the Brno Children Hospital's Gait Lab, University Hospital Brno

In this experiment, the VICON MX T020 system consisted of eight infrared cameras (height between 1.4m and 2.5m with frequency at 120 fps) that detected passive retro-reflexive markers placed on the human body (see Fig. 1) moving in a calibrated area (a 7m path). The system was calibrated before starting the experiment and recalibrated after each five examined volunteers. The double-step was chosen for analysis, as it is one of the most used step lengths among researchers [37]. Because the VICON system measured in 3D and was utilized due to its accuracy, the sagittal plane was monitored to obtain markers' precise signatures in 2D. This corresponded to the practical ideal situation when a person walks through a tunnel (or corridor), perpendicular to the camera (e.g. at airports, and laboratory conditions). The markers were set according to the Plug-In Gait Full-Body model (based on the Newington-Helen Hayes model) [38]. For this initial study, the following markers were selected (Fig. 1): the wrist bar on the side of the little finger (R(L)WRB), the second metatarsal head on the mid-sole side of the equinus break between fore-foot and mid-foot (R(L)TOE), the tibial wand on the lower third of the lower leg (R(L)TIB), the lower third surface of the thigh (R(L)THI), the acromio-clavicular joint (R(L)SHO), the lateral epicondyle (R(L)KNE), the heel (R(L)HEE), the lateral epicondyle approximating elbow joint axis (R(L)ELB), the anterior superior iliac spine points (R(L)ASI), and the lateral malleolus along the imaginary line passing through the transmalleolar axis (R(L)ANK).

Each volunteer was tested by walking on the path in the calibrated area (at least 10 times) in order to obtain data to prove or disprove whether different walking types had different effects on human body movement patterns:

- self-selected natural speed gait (NG),

- walking with slow music in the background (SM),

- walking with fast music in the background (FM),

- walking to the rhythm of a metronome (MM[1].92, MM.120, MM.144),

- walking after a 5-minute workout – deep squat (AW).

Recordings of each single walk were given, smoothed, filtered and exported to a csv software file for further pre-processing (selection of double-steps, extraction of erroneous data behaviour, time rescale, and for preparation of the whole dataset) in MS Excel. All further statistical analyses were performed using the R software, the FDA package.

Table 1. Basic characteristics and biometrics of participants in the study (mean ± standard deviation)

	Weight [kg]	Height [m]	Age [yrs.]	BMI
All	71.86± 16.41	1.79 ± 0.07	23.65 ± 2.62	22.35 ± 4.81
Women	59.57 ± 8.39	1.70 ± 0.02	25.67 ± 4.53	20.60 ± 3.09
Men	75.96± 12.56	1.82 ± 0.07	22.97 ± 1.57	22.94 ± 3.91

B. Functional Data Analysis

The Functional Data Analysis is the statistical-analytic technique utilized for this human gait behaviour (i.e. the curve created by walking) study [28]. In this approach, real time series data is treated as the function implying that all of the information is preserved in the data and not removed due to summarizing data to single numbers (mean, standard deviation, etc.), thus functional data analysis uses the entire sequence of individual measurements as a single functional entity. It is assumed that the gait signature is generated by an underlying function where discrete time-ordered measurements of the individual, acquired from special camcorders, are snapshots of this function. The responsive comparison between individuals' signatures is calculated by the functional one-way ANOVA (fANOVA) [29, 39].

The marker signature for the ith individual and for the rth replication arrives as the finite set of values

$$y_{ir}(t_1), y_{ir}(t_2), \ldots, y_{ir}(t_{n_r}), \qquad (1)$$

where

$$y_{ir}(t_j) = m_{ir}(t_j) - h_i. \qquad (1a)$$

Here $t_j \in T$ denotes the jth percentage point of the gait cycle for the ith subject, $i = 1, \ldots, 12$, in the rth replication, $r = 1, \ldots, 10$, $T = [0\%, 100\%]$ denotes the range of values of argument, n_r indicates the number of measured values for the ith individual in the rth replication, $m_{ir}(t_j)$ is

---

[1] The metronome's tempo is set by beats per minute (BPM) named as MM (Mälzel's metronome). Values of BPM and MM are equal.

the measurement captured by the VICON MX T020 system, and h_i is the height corresponding to the marker for the ith individual measured from the landmark to the floor. The height h_i eliminates the influence of the subject's height. The marker signature (1) is converted to the function y_{ir} computable for any value t by smoothing. The function y_{ir} is defined as the linear combination of K known basis functions $\{\Phi_1, \Phi_2, \ldots, \Phi_K\}$ and the error model is expressed as:

$$y_{ir}(t_j) = \sum_{k=1}^{K} c_{irk} \Phi_k(t_j) + \varepsilon_{ir}(t_j), \qquad (2)$$

$i = 1, \ldots, 12$, $r = 1, \ldots, 10$, $j = 1, \ldots, n_r$, where B-spline basis functions $\Phi_k, k = 1, \ldots, K$, are used, and the errors $\varepsilon_{ir}(t_j)$ are mutually independent with the zero mean and the unknown common constant variance. The number of basis functions K was selected by the stepwise variable selection procedure. The smoothing of raw discrete data was carried out using the penalized least squares approach. Coefficients c_{irk} were chosen to minimize the following expression

$$\sum_{i=1}^{12} \sum_{r=1}^{10} \sum_{j=1}^{n_r} \left[y_{ir}(t_j) - \sum_{k=1}^{K} c_{irk} \Phi_k(t_j) \right]^2 + \lambda PEN_2(\sum_{k=1}^{K} c_{irk} \Phi_k(t)), \qquad (3)$$

whereby $PEN_2(x) = \int [D^2 x(s)]^2 ds$ is the integrated squared second derivative and it penalizes the curvature of the estimated functions. The trade-off between how well the measurements fit to the data, and the lack of the smoothness was controlled by the smoothing parameter λ, whose value was chosen by generalized cross-validation. The resulting estimated smooth functions, which are further analysed, are:

$$y_{ir}^S(t) = \sum_{k=1}^{K} \hat{c}_{irk} \Phi_k(t), \qquad (4)$$

$i = 1, \ldots, 12, r = 1, \ldots, 10$, where $\hat{c}_{irk}$ denote the fitted coefficients defined by the minimizing criterion (3).

The effect individuals have on the movement pattern from the marker is investigated by the one-way fANOVA. In the one-way fANOVA, I groups of random functions $Y_{iR}(t)$, and $R = 1, \ldots, N_i$, defined over the bounded interval $T = [a, b]$, which are independent samples of the function $\mu_i(t)$, $i = 1, \ldots, I$, are analysed. The I-sample testing problem for functional data is the test of the equality of the mean functions, i.e. the null hypothesis is $H_0: \mu_1(t) = \cdots = \mu_I(t)$; $t \in T$, against the alternative that at least two mean functions are not equal. The test statistic of the omnibus test is defined as

$$F(t) = \frac{SSR(t)/(I-1)}{SSE(t)/(N-I)} = \frac{\sum_{i=1}^{I} N_i (\bar{Y}_{i.}(t) - \bar{Y}_{..}(t))^2/(I-1)}{\sum_{i=1}^{I} \sum_{R=1}^{N_i} (Y_{iR}(t) - \bar{Y}_{i.}(t))^2/(N-I)}, \qquad (5)$$

where $N = \sum_{i=1}^{I} N_i$, N_i is the number of the signatures for the ith individual, $\bar{Y}_{i.}(t) = \sum_{R=1}^{N_i} Y_{iR}(t)/N_i$ is the sample group mean function, $\bar{Y}_{..}(t) = \sum_{i=1}^{I} \sum_{R=1}^{N_i} Y_{iR}(t)/N$ is the sample grand mean function, $SSR(t)$ and $SSE(t)$ denote the point variations between-subject and within-subject, respectively. For testing H_0, the maximum value of $F(t)$ over T, denoted by F_{max}, is compared to the permutation-based critical value.

F_{max} values were calculated over selected percentages of the gait cycle $T_F = \{0\%, 1\%, 2\%, \ldots, 100\%\}$ with $N_i = 10$, $i = 1, \ldots, 12$, $N = 120$, and $Y_{iR}(t) = y_{ir}^S(t)$. The critical value of the resulting F_{max}-test was carried as follows: the indices ir were

permuted $P = 1000$ times and for each permutation p the values $\bar{Y}_{i.}^p(t)$, $\bar{Y}_{..}^p(t)$, and $F^p(t)$ were calculated at 101 equidistant percentages points of the gait cycle, and the value $F_{max}^p = \max\{F^p(t): t \in T_F\}$ was determined. The null hypothesis is rejected at the significance level α, if $F_{max} > c_{1-\alpha}$, where $c_{1-\alpha}$ is the $(1-\alpha)$-quantile of the empirical distribution of the maximal F-statistic values $F_{max}^1, F_{max}^2, \dots, F_{max}^{1000}$. When the null hypothesis is rejected, the functional Scheffé post hoc test can be used to detect the difference among all pairs of the mean functions. The two mean functions are significantly different at the significance level α if it holds

$$\left|\bar{Y}_{i.}(t) - \bar{Y}_{j.}(t)\right| > \{(I-1)c_{1-\alpha}\}^{1/2} \times \{SSE(t)(N-I)^{-1}(N_i^{-1} + N_j^{-1})\}^{1/2} \quad (6)$$

for a part of T.

III. RESULTS

A. FDA results

Table 2. Percentages of significantly different pairs of mean gait signatures; legend: NG – Normal gait, SM – Slow Music, FM – Fast Music, AW – After Workout

	NG	SM	FM	MM.92	MM.120	MM.144	AW	Mean
LANK	81.82	80.30	89.39	87.88	89.39	80.30	78.79	83.98
LASI	92.42	80.30	92.42	96.97	92.42	96.97	92.42	91.99
LELB	98.48	98.48	96.97	95.45	92.42	93.94	92.42	95.45
LHEE	84.85	78.79	77.27	80.30	87.88	90.91	83.33	83.33
LKNE	90.91	89.39	95.45	93.94	90.91	90.91	86.36	91.12
LSHO	95.45	96.97	95.45	98.48	96.97	100	95.45	96.97
LTHI	89.39	93.94	95.45	93.94	96.97	93.94	87.88	93.07
LTIB	87.88	87.88	87.88	98.48	89.39	89.39	81.82	88.96
LTOE	93.94	90.91	93.94	92.42	95.45	96.97	90.91	93.51
LWRB	96.97	92.42	92.42	98.48	89.39	83.33	90.91	91.99
RANK	83.33	90.91	93.94	87.88	90.91	92.42	80.30	88.53
RASI	86.36	89.39	92.42	96.97	93.94	90.91	95.45	92.21
RELB	95.45	98.48	100	100	96.97	95.45	87.88	96.32
RHEE	83.33	86.36	86.36	77.27	89.39	80.30	77.27	82.90
RKNE	78.79	80.30	78.79	87.88	87.88	87.88	84.85	83.77
RSHO	92.42	90.91	93.94	95.45	93.94	92.42	86.36	92.21
RTHI	95.45	92.42	89.39	93.94	93.94	95.45	90.91	93.07
RTIB	87.88	84.85	92.42	86.36	93.94	78.79	92.42	88.09
RTOE	93.94	95.45	89.39	93.94	92.42	95.45	96.97	93.94
RWRB	93.94	95.45	93.94	98.48	98.48	72.73	89.39	91.77
Mean	90.15	89.69	91.36	92.72	92.65	89.92	88.10	-

The significant difference (at the level $\alpha = 0.05$) of the mean signatures of all individuals was indicated over the whole set T_F (selected percentages of the gait cycle) for all markers, and for all examined walking speeds and conditions. To detect which pairs of mean signatures are significantly different (at the level $\alpha = 0.05$), Scheffé's functional procedure was used. Together (12×11)/2 shows that there are 66 possible contrasts of mean signatures analysed for all markers and all walking speeds and conditions (Table 2). All the markers under every walking condition significantly distinguished a high percentage of individual pairs (more than 72 %, i.e. at least 48 pairs from 66 were distinguished). On average, the R(L)ELB and LSHO were the best markers with the highest number of significantly different pairs of individuals;

conversely, the worst results were from the R(L)HEE, LANK and RKNEE. Discrimination of some markers was highly dependant on walking speeds and conditions, e.g. RWRB successfully distinguished 98 % of pairs for MM.92 and MM.120, however only 72 % was distinguished for MM.144. On average, the highest number of significantly different pairs of individuals was detected for MM.92 and MM.120.
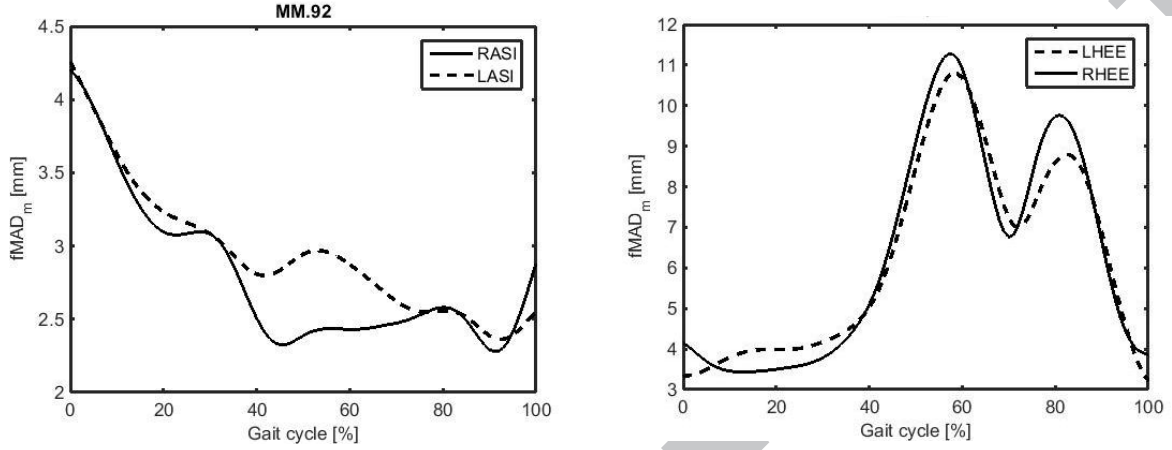

Figure 2. Example of functional mean absolute deviations (fMAD$_m$) for R(L)ASI (left) and R(L)HEE (right) for the walking speed MM.92

The quality of markers was further investigated by the variability of markers' trajectories. This was assessed through the sample functional mean absolute deviation (fMAD) from mean trajectories (averaged over all signatures for the given marker and the given walking speed and condition):

$$\text{fMAD}_m(t_l) = (12 \cdot 10)^{-1} \sum_{i=1}^{12} \sum_{r=1}^{10} |y_{ir}^S(t_l) - \bar{Y}_{i.}(t_l)|, \quad (7)$$

for $t_l \in T_F$. Functions fMAD$_m$ for the R(L)ASI and R(L)HEE for the walking speed MM.92 are shown in Fig. 2. It is visible that different markers under the same walking speed and condition lead to various functions fMAD$_m$. The highest values of the fMAD$_m$ for R(L)ASI signatures occurred over 0 % - 30 % of the gait cycle, while for R(L)HEE it was over 50 % - 90 % of the gait cycle. Furthermore, the averaged fMAD$_m$, i.e. fMAD$_m$ averaged over all percentages of the gait cycle, for R(L)HEE is more than twice as big as R(L)ASI (Table 3). As one can see in Table 3, the least variability of markers' signatures was found for R(L)ASI and R(L)KNE with averaged fMAD$_m$ which is about 3 mm for all walking paces and conditions. Deviations of the majority of markers' signatures varied from 3 to 5 mm. The biggest variability of trajectories was detected for R(L)WRB with averaged fMAD$_m$ varying from 6 mm to 15.45 mm depending on a walking pace and conditions. The results for NG, SM, FM, MM.92, and MM.120 are comparable on the average with the mean of averaged fMAD$_m$, which is about 4.5 mm.

Table 3. Sample averaged functional mean absolute deviations, averaged over all trajectories and percentages of the gait cycle (in mm); legend: NG – Normal gait, SM – Slow Music, FM – Fast Music, AW – After Workout

	NG	SM	FM	MM.92	MM.120	MM.144	AW	Mean
LANK	4.95	5.05	4.67	5.26	5.04	8.11	5.88	5.57
LASI	2.63	2.89	2.80	3.09	2.90	3.03	2.52	2.84
LELB	4.46	4.65	4.40	4.18	5.55	5.83	8.11	5.31

LHEE	5.16	5.91	5.66	6.49	5.94	8.45	7.63	6.46
LKNE	3.13	3.34	2.94	3.01	3.43	3.89	3.39	3.30
LSHO	3.36	3.65	3.41	3.10	3.75	3.50	4.64	3.63
LTHI	3.30	3.47	3.25	3.17	3.69	4.16	3.57	3.52
LTIB	4.47	4.69	4.68	4.68	4.82	6.22	5.82	5.05
LTOE	3.27	3.39	3.34	3.51	3.16	4.02	3.83	3.50
LWRB	8.76	8.54	8.50	8.02	10.26	15.45	12.82	10.34
RANK	5.29	5.53	4.35	5.12	5.41	8.29	5.96	5.71
RASI	2.57	2.80	2.41	3.05	3.21	3.10	2.62	2.82
RELB	5.02	4.98	4.52	5.30	4.76	5.36	8.20	5.45
RHEE	6.59	6.86	5.48	7.29	6.59	8.84	6.46	6.87
RKNE	2.89	3.24	2.94	3.03	3.51	3.45	3.37	3.20
RSHO	3.53	3.37	3.80	3.82	4.69	3.84	4.98	4.00
RTHI	2.88	3.35	3.03	3.12	3.62	4.60	3.52	3.45
RTIB	4.72	5.05	3.68	4.39	4.91	6.25	5.11	4.87
RTOE	3.64	3.42	3.75	3.27	3.61	4.37	3.58	3.66
RWRB	7.09	6.67	6.77	6.23	6.04	10.36	10.42	7.65
Mean	4.39	4.54	4.22	4.46	4.74	6.06	5.62	-

Although no individuals stated any problems in their muscular-skeletal system that affects their movement pattern, one can see slight differences between results obtained from markers on the left and markers on the right side of the body (Tables 2 - 4, Fig. 2). This points to a common issue in living organisms – slight asymmetry of bodies caused by their growth. Such discrepancies probably also relate to irregular human body movement patterns for some individuals. An individual was considered having an irregular movement pattern if the inequality

$$|y_{ir}^S(t_l) - \bar{Y}_{i.}(t_l)| > 3\text{fMAD}_m(t_l) \qquad (8)$$

was satisfied at least for one $t_l \in T_F$ in more than five trajectories (Table 4).

Almost all participants had a regular movement pattern or their irregularity occurred only for a few combinations of markers for some walking speeds and conditions. However, for the participant M7, irregularity in movement patterns was found in many markers for all walking speeds and conditions, except the movement pattern after the workout condition (AW). The variability of signatures for individuals can be analysed by means of the sample fMAD$_i$ (averaged over all signatures for the given individual, marker, walking speed and condition)

$$\text{fMAD}_i(t_l) = 10^{-1} \sum_{r=1}^{10} |y_{ir}^S(t_l) - \bar{Y}_{i.}(t_l)|, t_l \in T_F. \qquad (9)$$

The comparison of the sample fMAD$_i$ of RHEE signatures for M7 (identified as having irregular movement pattern with 7 signatures), M6 and M15 (not showing an irregular movement pattern with 4 and 0 signatures, respectively) for walking speed MM.92 is demonstrated in Fig. 3. It is visible that the fMAD$_i$ is very narrow and stable for M15, however for M7 the values fluctuate and are markedly higher at some percentages of the gait cycle.

Table 4. Individuals with irregular movement patterns (the sample functional absolute deviation is more than three-times the sample functional mean absolute deviation at least for one time in more than 5 signatures); legend: NG – Normal gait, SM – Slow Music, FM – Fast Music, AW – After Workout

	NG	SM	FM	MM.92	MM.120	MM.144	AW

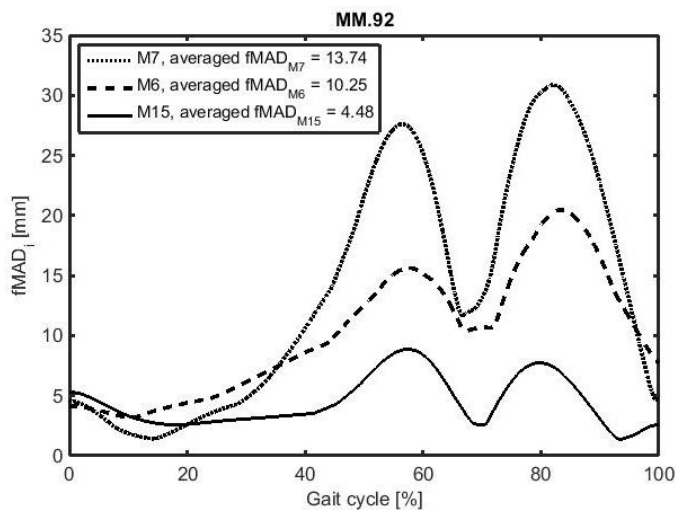|							
LANK	F6	M2	-	M7	-	M7	M11
LASI	M7,M6	-	M6	M7	-	-	-
LELB	M7	-	-	M7	F6	-	-
LHEE	-	-	-	-	-	-	M11
LKNE	-	-	-	M6	-	M7	M11
LSHO	M7	M6	-	M7	-	-	-
LTHI	-	-	-	-	-	-	-
LTIB	-	-	-	-	-	M7	M11
LTOE	-	M11	M9	M6	M6	-	-
LWRB	M12	M7,M6	F6	M7	M7, F6	M7	-
RANK	M7	M7	M7	M7	M7	M7	-
RASI	M7,M6	M7, F6	M6	M7	M7, M6	M6	-
RELB	M12	M7	M7	M7	M7	M12	-
RHEE	M7	M7	M7	M9, M7, F4	M7,M14	M7,M11	-
RKNE	-	F6	-	-	-	M6	-
RSHO	-	M7	-	M7	M12	-	-
RTHI	-	-	-	-	M6	M7	-
RTIB	M7	M7,M9	-	M7	M7, F6	M7	-
RTOE	-	M7,M6	M7,M6	M7,M6	M2	M12	M6,M2
RWRB	M12	F6	-	M12	-	M7,M12	-

Figure 3. Example of functional mean absolute deviations of individual M7, M6, and M15 for RHEE and for walking pace MM.92

B. *Performance evaluation for identifying individuals in 1:1 matching*

Identifying or verifying an individual has always been a security issue. The aim of such a system (e.g. biometric methods) is to faultlessly grant rights to authorized persons and to reliably detect and reject people without such rights. The rate of false acceptance (FAR) and the rate of false rejection (FRR) are used as the performance metrics for biometric systems. The ideal appliance has no failures or errors – 100 % of individuals are recognized, there is no FRR or FAR. The FAR and FRR in biometric authentication systems are set by choosing a particular detection threshold. By varying its value, one of the errors decreases, but the other error rate automatically increases and therefore the balance must be found. The receiver operating characteristics (ROC) curve is used to visualise the trade-off between the FRR and the FAR for possible values of the threshold. Youden's index may be used as a criterion for selecting the optimum value of the detection threshold. The equal error rate (EER), i.e. the point on the ROC curve where the FAR and FRR are equal, can also be used as the

performance metric to compare the accuracy of the systems (the closer to the inception in the graph, the smaller the error rate of the system). Hence, the lower the EER, the better the method performance.

The FRR and FAR were evaluated through the inequality (8), where the multiple of the $fMAD_m$ changes. Together, 120 gait signatures for each marker and walking condition were tested. The gait signature was considered different from the chosen pattern if the inequality (8) was satisfied at least at one point of the gait cycle. The FRR and FAR corresponding to the established thresholds, together with the EER, are presented in Table 5. The results are satisfactory and consistent with those obtained from the fANOVA. Again, one can see that values of the FRR, FAR and EER fluctuate for various markers and walking conditions. Some markers like R(L)ELB and LSHO provide good rates for the majority of walking conditions with FRR/FAR/EER less than 1.5/5/5 %. The impact of the walking conditions on gait recognition performance was deeply investigated by the ROC curves - see Fig. 4, where curves for the RELB and RWRB markers are demonstrated.

Table 5. FRR, FAR and EER values (in percent) obtained by utilizing the FDA method; legend: NG – Normal gait, SM – Slow Music, FM – Fast Music, AW – After Workout

		NG	SM	FM	MM.92	MM.120	MM.144	AW
LANK	FRR	0	3.63	1.19	4.56	0.83	6.97	3.99
	FAR	16.81	11.95	8.56	11.84	11.29	14.16	16.65
	EER	10.55	9.36	6.54	9.50	8.33	12.03	11.44
LASI	FRR	0	3.61	1.76	0	0	1.04	0
	FAR	16.66	18.13	10.91	6.50	8.95	7.85	9.59
	EER	9.80	13.25	7.63	3.62	6.58	5.99	6.20
LELB	FRR	0.83	1.67	0	0	0.83	1.97	1.04
	FAR	3.65	3.95	2.84	3.69	7.08	8.26	12.32
	EER	3.49	3.52	2.12	2.95	5.36	5.47	7.69
LHEE	FRR	3.73	3.78	7.15	4.46	1.85	2.38	5.29
	FAR	9.25	14.86	11.17	15.90	10.32	11.55	13.57
	EER	7.19	10.39	9.19	11.77	7.40	8.39	10.25
LKNE	FRR	0	5.01	0.83	0	1.76	3.84	2.31
	FAR	11.71	7.62	6.97	10.27	9.89	6.04	11.41
	EER	8.80	7.01	5.18	5.47	7.17	5.51	8.40
LSHO	FRR	1.19	4.47	2.31	0	0	0	0
	FAR	5,75	3.81	6.19	4.14	3.70	4.18	11.20
	EER	4.04	4.44	5.54	3.11	3.14	3.21	6.42
LTHI	FRR	2.86	0	2.71	2.59	2.08	0.83	3.52
	FAR	7.19	6.95	5.66	7.70	6.30	9.57	9.15
	EER	6.33	4.87	5.20	5.69	4.40	6.02	6.53
LTIB	FRR	0.83	2.11	1.04	0	0	4.56	3.30
	FAR	11.71	10.32	12.56	7.64	11.60	9.79	11.56
	EER	8.36	8.17	8.17	5.40	6.69	7.28	8.73
LTOE	FRR	1.04	0	4.08	0.92	1.04	1.04	4.79
	FAR	7.74	9.65	6.56	8.35	8.26	7.13	8.25
	EER	6.56	5.72	5.75	5.94	5.89	4.79	7.09
LWRB	FRR	0.93	0	1.76	5.60	0	9.45	2.59
	FAR	7.96	9.899	9.75	4.84	15.97	7.06	11.28
	EER	6.77	6.65	7.14	5.99	12.46	9.45	9.09
RANK	FRR	5.58	1.19	1.67	1.04	4.05	6.38	14.89
	FAR	11.35	15.05	6.73	11.83	9.28	8.24	7.67
	EER	9.25	9.05	5.62	8.67	7.20	7.70	12.31
RASI	FRR	1.04	5.42	2.92	0	2.23	0.93	1.97

	FAR	17.14	9.51	9.26	8.47	11.39	12.03	8.35
	EER	10.16	8.72	7.29	5.96	8.59	8.15	6.94
RELB	FRR	0.93	0	0	1.67	0	0	2.02
	FAR	9.03	5.54	4.35	1.49	3.22	7.97	14.89
	EER	6.81	3.53	2.92	1.67	2.85	4.74	9.72
RHEE	FRR	6.05	2.89	3.63	7.43	0	4.71	0.93
	FAR	13.29	13.70	5.38	15.21	10.38	9.35	20.06
	EER	10.83	8.59	5.15	12.05	6.91	7.87	11.62
RKNE	FRR	2.86	0.83	1.04	3.30	1.97	2.71	6.46
	FAR	13.46	17.84	18.80	13.04	12.16	10.63	13.22
	EER	9.64	9.72	11.27	8.86	8.94	7.71	11.95
RSHO	FRR	1.39	1.39	0.83	1.04	1.67	0	2.95
	FAR	10.48	10.59	7.33	7.72	6.94	13.18	13.11
	EER	8.52	6.97	5.71	6.32	5.77	8.49	9.46
RTHI	FRR	2.23	1.04	2.23	0	0	3.58	1.19
	FAR	2.58	5.66	11.62	7.22	8.69	10.01	9.20
	EER	2.56	5.17	7.51	4.30	6.67	7.74	6.93
RTIB	FRR	5.82	1.97	2.02	0.93	0	4.89	1.04
	FAR	8.88	11.33	6.51	9.19	8.20	18.13	10.25
	EER	7.83	8.08	5.75	6.77	6.33	13.98	7.60
RTOE	FRR	2.38	0.92	2.50	0	2.22	0	0
	FAR	7.42	4.62	6.67	4.37	7.53	7.60	5.72
	EER	6.36	3.94	5.51	3.34	6.53	4.64	4.06
RWRB	FRR	0	0	4.46	0	0	9.18	3.54
	FAR	11.69	7.11	5.51	3.37	2.69	12.01	9.60
	EER	7.13	4.50	5.18	2.21	2.22	11.47	7.23

Furthermore, as can be seen in Table 5, the FAR and FRR can be higher than acceptable for commercial (i.e. civilian) biometric applications in the case of some body parts (i.e. markers). On the other hand, the calculated rates show that this system is highly applicable for forensic science (the FAR is about 7.5 % or higher, and the FRR has a very low value) or commercial verification systems for security checks in high security buildings (the FRR is 7.5 % or higher, and the FAR has a very low value; examples are in Fig. 4). Similarly, the ROC curves may help choose proper marker sets (or body parts for video-based recognition) for certain biometric applications, depending also on supposed walking speed that will not negatively affect results, but will contribute to greater accuracy in the system.
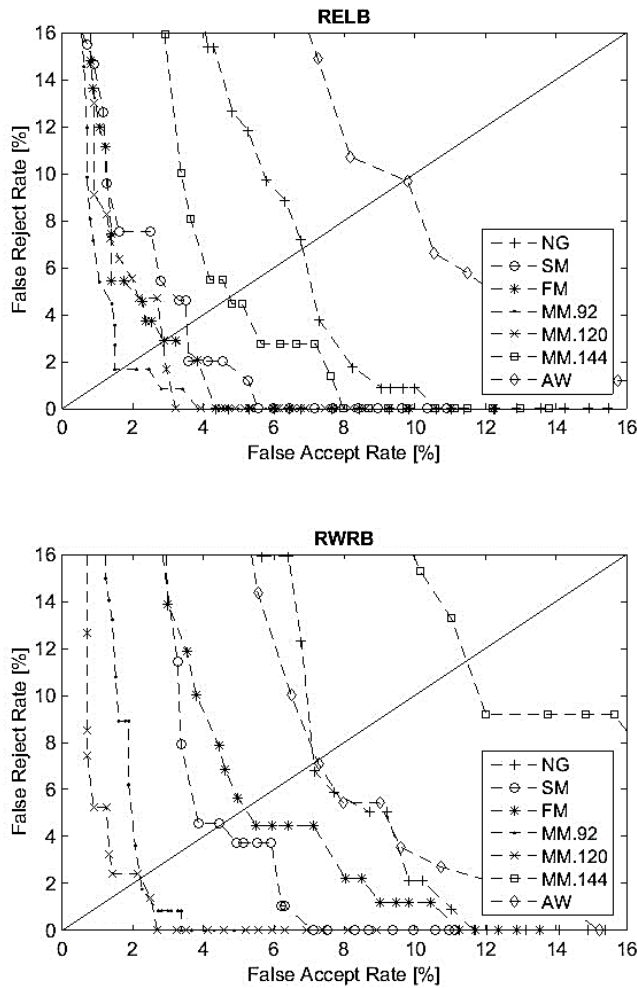
Figure 4. The ROC curves together with the EER for the RELB (upper panel) and RWRB (lower panel) markers under various walking conditions.

IV. DISCUSSION

The results obtained are statistically meaningful in terms of the methodology used and the results show proper identification and distinguishing among individuals. The most important markers on the human body are those placed on the biggest joints. Together with other selected markers, they form an exact picture of human body movement, and provide an excellent insight into the entire kinetics of the body. Furthermore, the approach presented incorporates differences in body height to the selected model in order to prevent undesired results based on different heights, in contrast to classical statistical analysis used in [12]. Therefore, the FDA provides accurate and reliable results needed in security (biometric) applications. The performance evaluation of this method shows promise and there are many potential applications in the real world e.g. as standard access control (1:1 matching), or for individual screening at airports or banks to detect suspects (1:N matching). The FDA is also applicable to real world applications where the person monitored is not fitted with markers,

but the whole procedure is based on video recognition/identification via a surveillance system. These systems are well worth further performance evaluation.

The main issue for utilizing this methodology in security applications (e.g. biometrics) is to realise how different conditions influence people's human body movement, i.e. how constant or chaotic the walking pattern is under different conditions, and consequently how these variations affect distinguishing among individuals. So far, several studies have focused on how clothes [42] or shoes [6,43] influence the whole identification process, but there are no studies focusing on various walking speeds. As the results show, the biggest difference is mainly in the movement of the upper body segments (i.e. shoulders and elbows) due to their dynamic movement during walking, while the behaviour of lower body segments (e.g. the knees and the ankles) is more constant because there is not much scope for extra movement.

Selected conditions were chosen to cover the most common types of movement. Using the metronome simulated different walking speeds from the slowest walk (slow promenade walk) to an extremely fast one, which nearly approached running. The purpose of deep squatting was to involve the thigh muscles whose weight affects the walk of the individual. This was also confirmed in results' evaluation. Incorporating music as a background was used to induce a relaxing atmosphere (for slow music) or a rousing mood (for fast music). This step was taken due to the large number of people listening to music in public, implying the necessity to also study such influences. Slight changes in the walking behaviour of volunteers were already visible during laboratory measurements as music (beats, respectively) has a relatively large influence on the overall gait signature. Also, an interesting result is how similar the fast music walking signature is with the normal gait of most of our volunteers. The biggest change in walking patterns can be seen in cases of very fast or very slow beats given by the metronome. The ideal speed for distinguishing among individuals is given by the walking speed equal to MM.92 and MM.120.

The challenge in further research is to apply this methodology to the dataset of more than 250 individuals (and ideally more than 1000) to see how appropriate this type of biometrics is, because there is a great possibility of people's information being put into a large database. Even though it seems that each individual has their own characteristic gait, variability of gait signatures in a large database may not be so high as to prevent correctly distinguishing among individuals with reasonable accuracy. This needs to be further verified in a large dataset by the FDA, which can prove its efficacy on this type of data and issues. For the moment, gait biometrics recognition/identification is suitable only for small applications with 1:1 matching.

V. CONCLUSION

The presented study is a pilot study focusing on human body movement, aimed at answering questions concerning the existence of gait signatures, the possibility to distinguish individual pairs or 1:1 individual identification by gait signatures, the affects of walking speed and various conditions, and marker positions for human body movement patterns. Therefore, 2D data (the sagittal plane only) instead of 3D data were used, which partly simplified the whole evaluating process. Furthermore, this situation is closer to the general video analysis where the human movement's record is not ideal, nor 3D, but it is ideal in a direction toward the camera. Even though some previous research in the gait recognition field worked with larger

databases (more than 100 participants [40-41]), results and databases mainly focused only on specific body parts and not whole bodies. Therefore, this small pilot study of 12 participants was undertaken to answer some issues that arose from previous studies.

Therefore, this paper introduces results from the initial study focussed on the appropriateness of human body movement (i.e. bipedal locomotion or gait) analysis, with the main focus on proving the affect of different walking speeds and conditions on an individual's gait signature. To study this issue properly, the functional data analysis methodology was employed as most suitable.

As expected, results showed that all markers under any walking speed and condition significantly distinguished a high percentage of individual pairs, and also that the quality of some markers characterized by the variability of marker signatures is highly dependent on walking speed and conditions. As for this, the most suitable walking speed for further analyses is the metronome speed MM.92 or MM.120. These walking speeds correspond with the average highest number of significantly different pairs of individuals on the one hand, and with the appropriate variability of marker signatures on the other hand. The least signature variability was found for markers on legs (R(L)ASI and R(L)KNE), with the average functional mean absolute deviation about 3 mm compared to the average functional mean absolute deviation of all markers of about 4.8 mm. The biggest variability in body movement signatures occurs in the case of the wrist marker, where it has, predictably, the highest volatility. Also, this methodology supports the issue of a slight asymmetry in the motion and growth of some participants, while most volunteers move relatively regularly even with asymmetric body proportions.

The gait analysis performance evaluation of the proposed methodology is promising and there is potential for applications in the real world. This method may help properly distinguish and identify individuals by their marker signatures. For example, this method can be a useful tool for physicians for identifying asymmetry in human locomotion, which can cause many health problems and heightens the probability of falls for elderly people. It is necessary to continue human body movement research, especially for the forensic science part of applications, where more testing is crucially necessary to provide highly accurate and reliable methods that will overcome human body movement asymmetries, body disproportions, and changes in walking speed under various background conditions or illness-based changes. The possibility of utilizing human body movements (gait) as a biometric feature still needs researching. For the moment, gait biometrics (recognition and/or identification) is suitable only for small applications with 1:1 matching.

VI. ACKNOWLEDGEMENTS

VII. REFERENCES

[1] A.K. Jain, A. Kumar, Biometric Recognition: An Overview, Second Gener. Biometrics Ethical, Leg. Soc. Context. (2012) 49–79. doi:10.1007/978-94-007-3892-8_3.

[2] D. Ioannidis, D. Tzovaras, I.G. Damousis, S. Argyropoulos, K. Moustakas, Gait recognition using compact feature extraction transforms and depth information, IEEE Trans. Inf. Forensics Secur. 2 (2007) 623–630. doi:10.1109/TIFS.2007.902040.

[3] S.R. Simon, Quantification of human motion: Gait analysis - Benefits and limitations to its application to clinical problems, J. Biomech. 37 (2004) 1869–1880. doi:10.1016/j.jbiomech.2004.02.047.

[4] M.F. Nowlan, Human Identification via Gait Recognition Using Accelerometer Gyro Forces, New Haven, Connecticut, 2009. Online [cit. 08/03/2017] <http://diyhpl.us/~bryan/papers2/paperbot/f6d49c0a2cbbfeb2453e4f18167ccd2b.pdf>.

[5] M. Iosa, A. Fusco, G. Morone, S. Paolucci, Development and decline of upright gait stability., Front. Aging Neurosci. 6 (2014) 14. doi:10.3389/fnagi.2014.00014.

[6] S. Mohammed, A. Samé, L. Oukhellou, K. Kong, W. Huo, Y. Amirat, Recognition of gait cycle phases using wearable sensors, Rob. Auton. Syst. 75 (2016) 50–59. doi:10.1016/j.robot.2014.10.012.

[7] C.T. Bonnet, A. Delval, L. Defebvre, Parkinson's Disease-Related Impairments in Body Movement, Coordination and Postural Control Mechanisms When Performing 80° Lateral Gaze Shifts., IEEE Trans. Neural Syst. Rehabil. Eng. 23 (2015) 849–56. doi:10.1109/TNSRE.2014.2369455.

[8] D. Rosenbaum, F. Macri, F.S. Lupselo, O.C. Preis, Gait and function as tools for the assessment of fracture repair - The role of movement analysis for the assessment of fracture healing, Injury. 45 (2014) S39–S43. doi:10.1016/j.injury.2014.04.007.

[9] E. Barrey, Methods, applications and limitations of gait analysis in horses., Vet. J. 157 (1999) 7–22. doi:10.1053/tvjl.1998.0297.

[10] L. Wang, U. Culha, F. Iida, A dragline-forming mobile robot inspired by spiders., Bioinspir. Biomim. 9 (2014) 16006. doi:10.1088/1748-3182/9/1/016006.

[11] H.M. Alawar, H. Ugail, M. Kamala, D. Connah, The Bradford Multi-Modal Gait Database: Gateway to Using Static Measurements to Create a Dynamic Gait Signature, Br. J. Appl. Sci. Technol. 14 (2016). doi:10.9734/BJAST/2016/13426.

[12] H.M. Alawar, H. Ugail, M. Kamala, D. Connah, The relationship between 2D static features and 2D dynamic features used in gait recognition, Proc. SPIE. 8712 (2013) 87120I–87120I–9. doi:10.1117/12.2015634.

[13] L. Wang, T. Tieniu, H. Ning, W. Hu, Silhouette Analysis-Based Gait Recognition for Human Identification, (n.d.).

[14] M. Hofmann, S. Sural, G. Rigoll, Gait Recognition in the Presence of Occlusion: A New Dataset and Baseline Algorithms, (n.d.).

[15] Y. Makihara, D.S. Matovski, M.S. Nixon, J.N. Carter, Y. Yagi, Gait Recognition: Databases, Representations, and Applications, (n.d.).

[16] M. Balážia, Human Gait Recognition Based on Body Component Trajectories, Masaryk University, 2013. http://is.muni.cz/th/256078/fi_m/thesis.pdf (accessed November 25, 2016).

[17] B. DeCann, A. Ross, J. Dawson, Investigating gait recognition in the short-wave infrared (SWIR) spectrum: dataset and challenges , in: 2013: p. 87120J–87120J–16. http://dx.doi.org/10.1117/12.2018145.

[18] H.J. Woltring, E.B. Marsolais, Optoelectric (Selspot) Gait Measurement in Two- and Three-Dimensional Space - a Preliminary Report, Bull. Prosthet. Res. 17 (1980) 46–52. http://www.ncbi.nlm.nih.gov/pubmed/7260460.

[19] S. Jaberzadeh, S. Scutter, M. Zoghi, Accuracy of an electromagnetic tracking device

for measuring hip joint kinematics during gait: effects of metallic total hip replacement prosthesis, source-sensor distance and sensor orientation, Australas. Phys. Eng. Sci. Med. 28 (2005) 184–189. doi:10.1007/BF03178714.

[20] D. Tzovaras, Activity Recognition: Gait Analysis and Recognition, Cent. Res. Technol. - Hellas Informatics Telemat. Inst. (2009) 85. Online [cit. 08/03/2017] <http://www.iti.gr/iti/files/document/seminars/Activity_recognition_final.pdf>.

[21] H.M. Clayton, H.C. Schamhardt, Measurement Techniques for Gait analysis, Equine Locomot. (2001) 55–76.

[22] J.E. Boyd, J.J. Little, Biometric gait recognition, Adv. Stud. Biometrics. (2005) 19–42. doi:10.1007/11493648_2.

[23] M.A. Pepper, Biometrics - A Perspective and a Case Study, New Zeal. Secur. (2002) 1–5.

[24] L. Amoore, Biometric borders: Governing mobilities in the war on terror, Polit. Geogr. 25 (2006) 336–351. doi:10.1016/j.polgeo.2006.02.001.

[25] K. Sulovska, S. Belaskova, M. Adamek, Gait Patterns for Crime Fighting: Statistical Evaluation, in: D. Burgess, G. Owen, R. Zamboni, F. Kajzar, A.A. Szep (Eds.), Proc. SPIE, Opt. Photonics Counterterrorism, Crime Fight. Def. IX; Opt. Mater. Biomater. Secur. Def. Syst. Technol. X, SPIE, 2013: p. UNSP 89010G-UNSP 89010G. doi:10.1117/12.2033323.

[26] W.A. Stuberg, V.L. Colerick, D.J. Blanke, W. Bruce, Comparison of a clinical gait analysis method using videography and temporal-distance measures using 16-mm cinematography, Phys. Ther. 68 (1988) 1221–1225.

[27] S. Zheng, J. Zhang, K. Huang, R. He, T. Tan, Robust view transformation model for gait recognition, in: Proc. - Int. Conf. Image Process. ICIP, 2011: pp. 2073–2076. doi:10.1109/ICIP.2011.6115889.

[28] N. Coffey, A.J. Harrison, O.A. Donoghue, K. Hayes, Common functional principal components analysis: a new approach to analyzing human movement data., Hum. Mov. Sci. 30 (2011) 1144–66. doi:10.1016/j.humov.2010.11.005.

[29] J.O. Ramsay, B.W. Silverman, Functional Data Analysis, Springer S, Springer Science+Business Media, New York, New York, 2005. doi:10.1007/978-0-387-98135-2.

[30] R. Baker, Gait analysis methods in rehabilitation, J. Neuroeng. Rehabil. 3 (2006) 10. doi:10.1186/1743-0003-3-4.

[31] E. Seminati, F. Nardello, P. Zamparo, L.P. Ardigo, N. Faccioli, A.E. Minetti, Anatomically Asymmetrical Runners Move More Asymmetrically at the Same Metabolic Cost, PLoS One. 8 (2013) 8. doi:10.1371/journal.pone.0074134.

[32] G.A. Bekey, C.-W. Chi-Wu Chang, J. Perry, M.M. Hoffer, Pattern recognition of multiple EMG signals applied to the description of human gait, Proc. IEEE. 65 (1977) 674–681. doi:10.1109/PROC.1977.10546.

[33] Z. Zhang, M. Hu, Y. Wang, A survey of advances in biometric gait recognition, Lect. Notes Comput. Sci. (Including Subser. Lect. Notes Artif. Intell. Lect. Notes Bioinformatics). 7098 LNCS (2011) 150–158. doi:10.1007/978-3-642-25449-9_19.

[34] R.D. Seely, On a three-dimensional gait recognition system by, University of Southampton, 2010.

[35] D.M. Gavrila, The Visual Analysis of Human Movement: A Survey, Comput. Vis. Image Underst. 73 (1999) 82–98. http://www.idealibrary.com (accessed October 24, 2016).

[36] R. Rak, V. Matyáš, Z. Říha, Biometrie a identita člověka ve forenzních a komerčních aplikacích, Grada, 2008.

[37] N. V. Boulgouris, D. Hatzinakos, K.N. Plataniotis, Gait Recognition: A challenging

signal processing technology for biometric identification, IEEE Signal Process. Mag. 22 (2005) 78–90. doi:10.1109/MSP.2005.1550191.

[38] C. Kirtley, Clinical Gait Analysis: Theory and Practice, 1st ed., Churchill Livingstone, 2003.

[39] J. Ramsay, G. Hooker, S. Graves, Functional Data Analysis with R and MATLAB, Springer New York, New York, NY, 2009. doi:10.1007/978-0-387-98185-7.

[40] S. Zheng, J. Zhang, K. Huang, R. He, T. Tan, Robust View Transformation Model For Gait Recognition, (n.d.).

[41] R. Vera-Rodriguez, J.S.D. Mason, J. Fierrez, J. Ortega-Garcia, Comparative Analysis and Fusion of Spatiotemporal Information for Footstep Recognition, IEEE Trans. Pattern Anal. Mach. Intell. 35 (2013) 823–834. doi:10.1109/TPAMI.2012.164.

[42] M.A. Hossain, Y. Makihara, J. Wang, Y. Yagi, Clothing-invariant gait identification using part-based clothing categorization and adaptive weight control, Pattern Recognit. 43 (n.d.) 2281–2291. doi:10.1016/j.patcog.2009.12.020.

[43] C.M. Kanzler, J. Barth, A. Rampp, H. Schlarb, F. Rott, J. Klucken, B.M. Eskofier, Inertial sensor based and shoe size independent gait analysis including heel and toe clearance estimation, in: 2015 37th Annu. Int. Conf. IEEE Eng. Med. Biol. Soc., IEEE, 2015: pp. 5424–5427. doi:10.1109/EMBC.2015.7319618.